

CONF-910715-48

Received by OSTI

Molecular to Material Design for Anomalous-Dispersion Phase-Matched Second Harmonic Generation 85206 1991

P. A. Cahill and D. R. Tallant

Sandia National Laboratories, Albuquerque, NM 87185

SAND--91-1551C

T. C. Kowalczyk and K. D. Singer

DE91 017999

Case Western Reserve University, Cleveland, OH 44106

## ABSTRACT

Anomalous-dispersion phase-matching (ADPM) offers large enhancements in the effective hyperpolarizabilities of nonlinear optical processes such as second harmonic generation (SHG) in organic materials. The principal barrier to the practical application of this approach is the residual absorption of asymmetric organic chromophores at the second harmonic which is shown by calculation to inherently limit the efficiency of SHG. Resonance Raman experiments on a nonlinear optical (NLO) dye optimized for doubling 800 nm light indicate that the residual absorbance is probably due to vibronic levels associated with the electronic absorption. Recent work with thin films of PMMA doped with this ADPM dye showed zero dispersion at approximately 6% concentration.

## 1. INTRODUCTION

Enhancement of the useful nonlinearity of organic and inorganic materials continues to be an important theme in the development of new second order NLO materials. Considerable success has been achieved in both inorganic (e.g. KTP) and organic materials (many examples of both crystals and thin films) for both second harmonic generation (SHG) and the linear electrooptic (LEO) effect. For SHG in particular, there exists a fundamental trade-off between the transparency of the NLO chromophore due to the wavelength of the first electronic absorption and the magnitude of its hyperpolarizability. The approach that we have taken has been to use organic chromophores that are very nearly transparent at energies above that of the first excited state and by doing so enhance the effective nonlinearity of the materials.

The possibility of such an enhancement was demonstrated by early electric field induced second harmonic generation (EFISHG) experiments with Foron Brilliant Blue S-R (FBB) in which the anomalous dispersion associated with this dye balanced the dispersion of the host solvent at an experimentally determined concentration.<sup>1</sup> Anomalous dispersion, which is the decrease in refractive index associated with an absorption, had first been suggested as a phase matching technique 30 years ago, but had only been investigated significantly for third order materials.<sup>2</sup> In this technique, the anomalous dispersion associated with one component of a mixture is used to cancel the normal dispersion of a second component, so that at a certain concentration the effective indices of refraction at the fundamental and the selected harmonic are equal, i.e., a phase-matched condition exists. Such an approach has been particularly successful for third harmonic generation in gas mixtures.<sup>3</sup>

The enhancement of the effective nonlinearity of anomalous-dispersion phase-matched (ADPM) materials specifically for SHG is derived from several factors. Some of the factors are geometric: that the second harmonic is collinear with the fundamental and that in a waveguide, both the fundamental and harmonic can exist in the lowest order modes. These geometric factors can significantly increase the degree of overlap of the propagating beams, thereby maximizing energy transfer for a given thickness of material. Possibly more significant factors are derived from the behavior of the microscopic hyperpolarizability ( $\beta$ ) of organic NLO chromophores as a function of wavelength. Based on a simple two-level model, an expression for  $\beta$  can be derived from perturbation theory which indicates that  $\beta$  increases as the square of the wavelength of the electronic transition. Because in ADPM SHG the energy of the electronic transition is less than the second harmonic (i.e., the NLO chromophore absorbs between  $\omega$  and  $2\omega$ ) rather than greater than the second harmonic (absorbing above  $2\omega$ ), an order of magnitude increase in  $\beta$ , and corresponding increases in the size of the corresponding macroscopic hyperpolarizability  $\chi^{(2)}$ , have been demonstrated. Furthermore, since the efficiency of SHG is proportional to  $[\chi^{(2)}]^2$ , extremely large (100-10,000) increases in the effective efficiency of SHG may be expected.

**MASTER**  
DISTRIBUTION OF THIS DOCUMENT IS UNLIMITED

## DISCLAIMER

This report was prepared as an account of work sponsored by an agency of the United States Government. Neither the United States Government nor any agency thereof, nor any of their employees, makes any warranty, express or implied, or assumes any legal liability or responsibility for the accuracy, completeness, or usefulness of any information, apparatus, product, or process disclosed, or represents that its use would not infringe privately owned rights. Reference herein to any specific commercial product, process, or service by trade name, trademark, manufacturer, or otherwise does not necessarily constitute or imply its endorsement, recommendation, or favoring by the United States Government or any agency thereof. The views and opinions of authors expressed herein do not necessarily state or reflect those of the United States Government or any agency thereof.

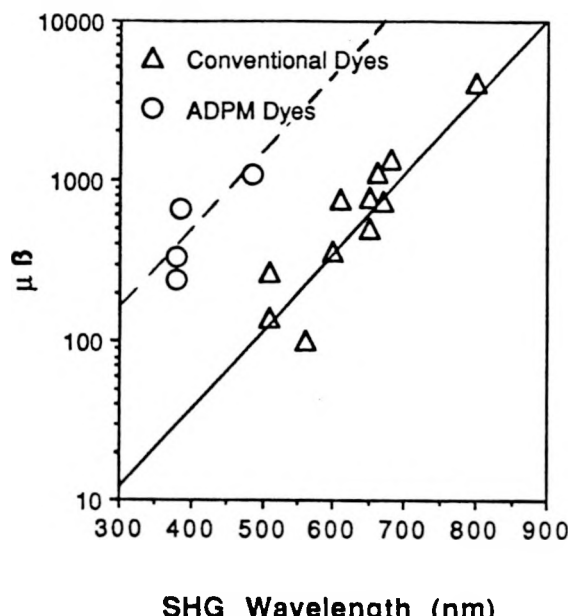
## DISCLAIMER

Portions of this document may be illegible in electronic image products. Images are produced from the best available original document.

## **DISCLAIMER**

This report was prepared as an account of work sponsored by an agency of the United States Government. Neither the United States Government nor any agency thereof, nor any of their employees, makes any warranty, express or implied, or assumes any legal liability or responsibility for the accuracy, completeness, or usefulness of any information, apparatus, product, or process disclosed, or represents that its use would not infringe privately owned rights. Reference herein to any specific commercial product, process, or service by trade name, trademark, manufacturer, or otherwise does not necessarily constitute or imply its endorsement, recommendation, or favoring by the United States Government or any agency thereof. The views and opinions of authors expressed herein do not necessarily state or reflect those of the United States Government or any agency thereof.

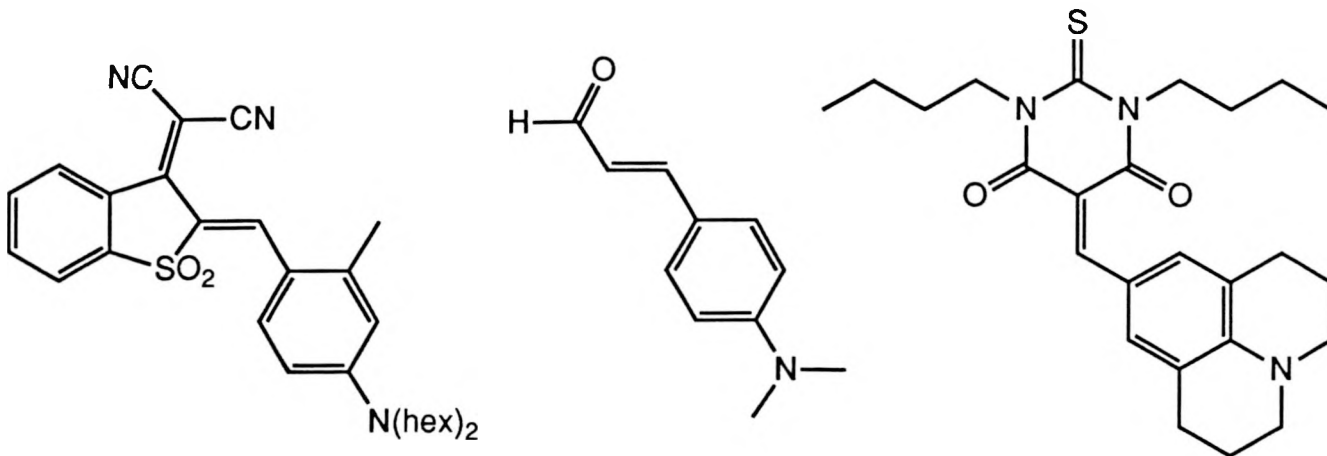
This is shown graphically in the chart below in which the  $\mu\beta$  product for several dyes has been plotted as a function of the UV cut-off wavelength for second harmonic generation. Conventional dyes, i.e., those in which the first electronic absorption is at higher energy than the second harmonic, generally fall along a line that indicates that the  $\mu\beta$  product decreases rapidly with decreasing wavelength. [This type of correlation has been reported by several research groups and may be attributed to the physics of second order nonlinear properties of molecules via perturbation theory.] The effective  $\mu\beta$  product of ADPM dyes tends to fall in the upper left hand quadrant of this chart. This is a direct result of using dyes which have their first electronic transition at a lower energy than the second harmonic, i.e., between the fundamental and second harmonic. The observed enhancement is approximately a factor of ten in  $\mu\beta$ .



## 2. STRUCTURE-PROPERTY RELATIONSHIPS OF ADPM CHROMOPHORES

The residual absorbance of the NLO dye at  $2\omega$  limits the efficiency (vide infra) and practicality of operating with a material above the energy of the first electronic transition. In typical organic molecules the absorbance due to molecular vibrations and their overtone and combination bands are often well separated both from other vibrational and electronic absorptions, but electronic absorptions are generally not well separated from each other. This gives rise in typical dyes to strong absorbance beginning in the visible region of the optical spectrum and continuing through the ultraviolet. There are exceptions to this general observation, e.g., in squaraines, some cyanine and related dyes, phthalocyanines, etc. These molecules, as a rule, do not have charge transfer type electronic absorptions, and therefore cannot be the NLO-active chromophore in second order based NLO devices.

Asymmetric (charge transfer) dyes with extremely low residual absorption are rare, but have been the focus of research at Sandia. FBB is a disperse dye with an unusually low residual absorbance to the blue shifted from the main (630 nm) absorption feature. This dye was used to demonstrate the ADPM SHG phenomenon, but its residual absorbance is much too high. Systematic variations on the basic chromophore dimethylaminocinnamaldehyde indicated that structurally rigid chromophores tended to yield dyes with lower residual absorption (normalized to the intensity of the principal electronic absorption band). Thus julolidinyl based donors nearly always gave better dyes for ADPM SHG. The relationship between the structure of the acceptor of the chromophore and the residual absorption is not clear. By trial and error, we discovered that the 2-thiobarbituric acid type of acceptor gave the best results. The dye X-523 combines the best donor and acceptor groups.



Foron Brilliant Blue S-R

Dimethylaminocinnamaldehyde

X-523

### 3. RESONANCE RAMAN EXPERIMENTS

In order to investigate the origin of the residual absorbance in dyes optimized for ADPM SHG, we undertook a Resonance Raman study of the di-n-butyl derivative of the julolidine/2-thio-pyrimidine trione dye designated X-523 (maximum absorbance at 523 nm in  $\text{CH}_2\text{Cl}_2$ ). Resonance Raman techniques are used to examine vibrational modes that are coupled to an electronic absorption. By examining how the Raman spectra vary with excitation wavelength, we anticipated learning which (and to what degree) vibrational modes couple to the electronic transition at 523 nm in order to aid in the design and synthesis of dyes with less residual absorption.

The experiments were performed under conditions in which no detectable decomposition of the dye occurred. Resonance Raman experiments were carried out with a 5 mW argon laser at 514.5 (very near resonance), 496.5, 488.0, and 457.9 nm (progressively off resonance to the blue) that was focussed onto a  $0.1 \times 2$  mm strip on the surface of a cuvette containing a fresh  $\text{CH}_2\text{Cl}_2$  solution of X-523. Nonresonant Raman spectra of X-523 at 647.1 nm (Krypton laser) were also taken in a nearly saturated  $\text{CH}_2\text{Cl}_2$  solution to maximize signal to noise. Significant fluorescence was observed at all wavelengths and was removed from the presented spectra by a polynomial fitting procedure. Stokes/anti-Stokes line intensities indicated that the spectroscopic temperature of the dye and the solution were not significantly different from room temperature. In all cases the solvent contributed lines to the spectra at 288, 704, 743, 1155, and  $1420 \text{ cm}^{-1}$  which become increasingly noticeable in the off-resonant spectra. The remaining lines in Figure 1 are therefore assigned to X-523.

In Figures 2 and 3, Raman spectra of X-523 solutions are compared with Raman spectra of julolidine, 1,3-dimethyl barbituric acid, and 1,3-diethyl-2-thiourea. The spectra of the dye and julolidine are similar from approximately  $1000 \text{ cm}^{-1}$  to  $1600 \text{ cm}^{-1}$ . The most intense bands in this region are believed to be due to the aromatic fragment of these molecules. The difference in band frequencies between X-523 and julolidine in this region may be due to the difference in the conjugation lengths of the double bonds in the compounds. The highest frequency ( $1623 \text{ cm}^{-1}$ ) band in the X-523 spectrum is at too high a frequency for a carbon-carbon double bond, especially a conjugated one. It is more likely due to a carbonyl ( $\text{C}=\text{O}$ ) vibration, similar to the one yielding the band near  $1700 \text{ cm}^{-1}$  in the barbituric acid spectrum. There is no distinct Raman band due to the  $\text{C}=\text{S}$  in the X-523 spectrum. This band occurs near  $730 \text{ cm}^{-1}$  in thiourea derivatives.<sup>4</sup> Note that the dye so strongly absorbs at 514.5 nm that solvent bands are not detectable in the lower spectrum of Figure 3. Only the resonance-enhanced bands of the dye are present at intensities distinguishable from the noise level.

The resonance-enhanced Raman bands of X-523 appear to be related to the carbonyl groups of the barbituric acid component and to the aromatic group of the julolidine component. This is consistent with the assignment of the electronic

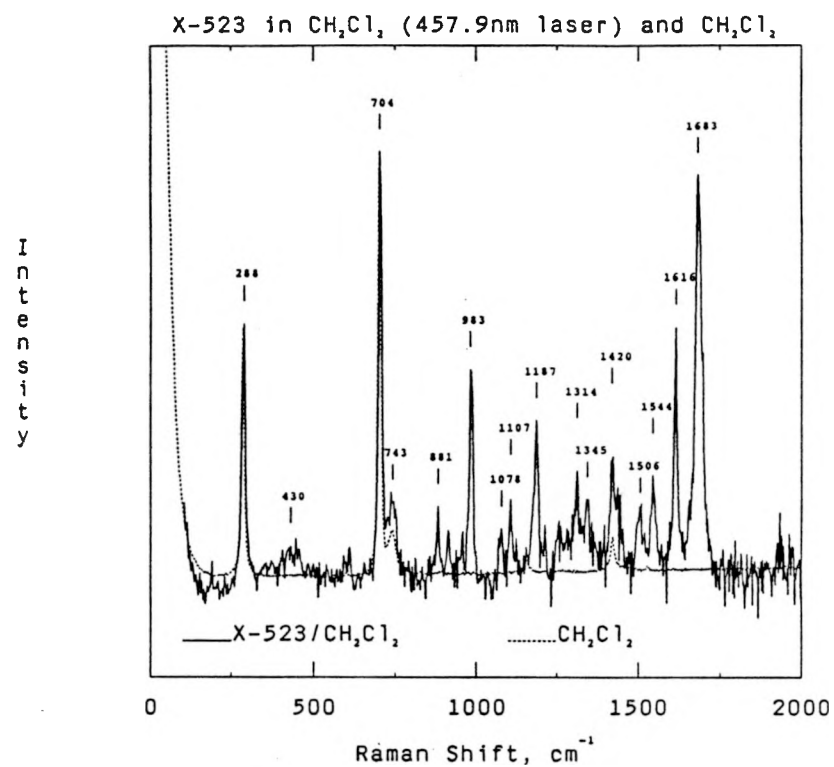


Figure 1. Resonance Raman spectrum of NLO dye X-523 in methylene chloride.

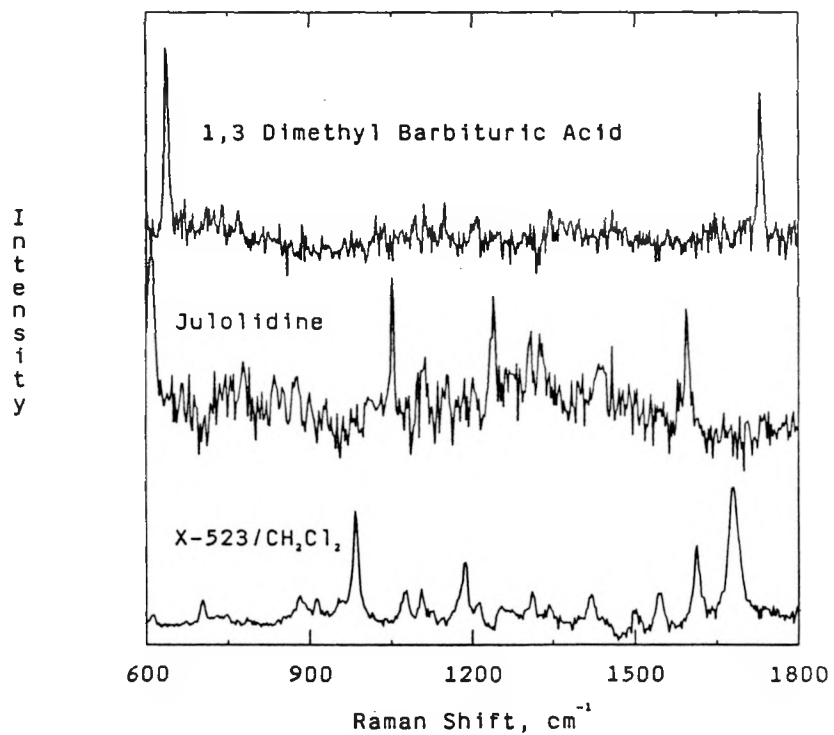


Figure 2. Comparison of Raman spectra of X-523 with spectra of molecules related to its molecular fragments. Note the shifts in both the carbonyl (C=O) stretch of the barbituric acid near  $1700 \text{ cm}^{-1}$ , and in the ring modes of the julolidine between  $1200$  and  $1600 \text{ cm}^{-1}$ .

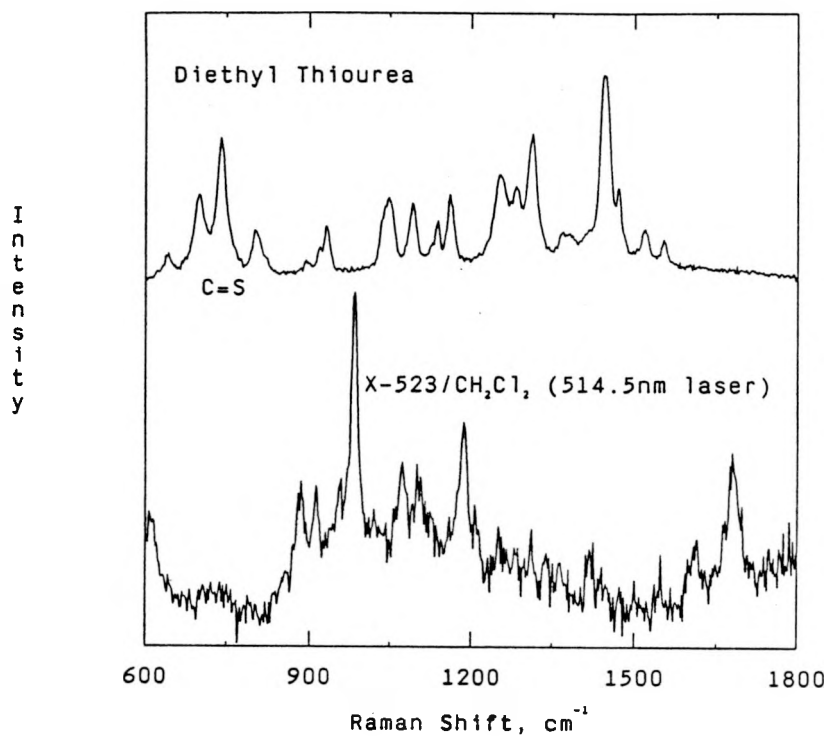


Figure 3. Comparison of Raman spectra of X-523 with thiourea. Note the absence of a C=S mode in X-523's spectrum.

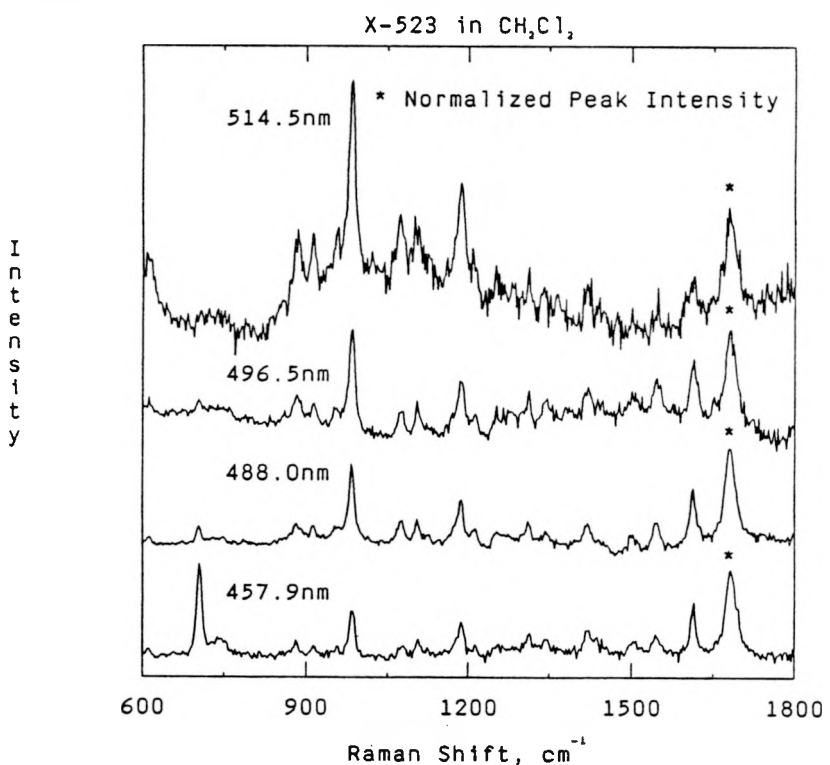


Figure 4. Resonance Raman spectra of X-523 at given wavelengths, normalized to the intensity of the 1683 cm<sup>-1</sup> (C=O) absorption. Note the change in relative intensities as a function of irradiation wavelength.

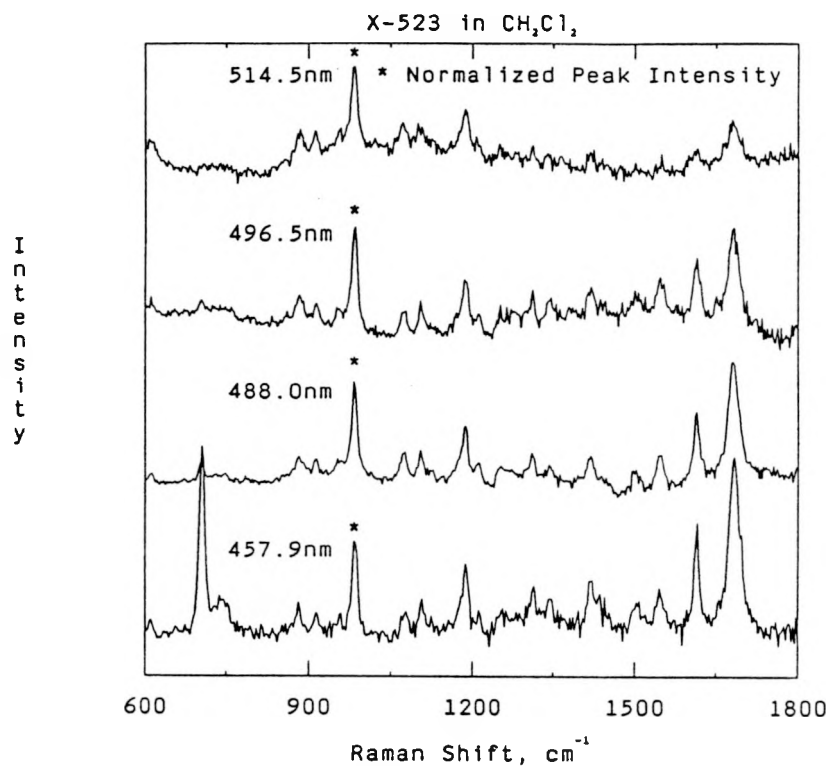


Figure 5. The same data as Figure 4, but normalized to the intensity of the  $983 \text{ cm}^{-1}$  absorption.

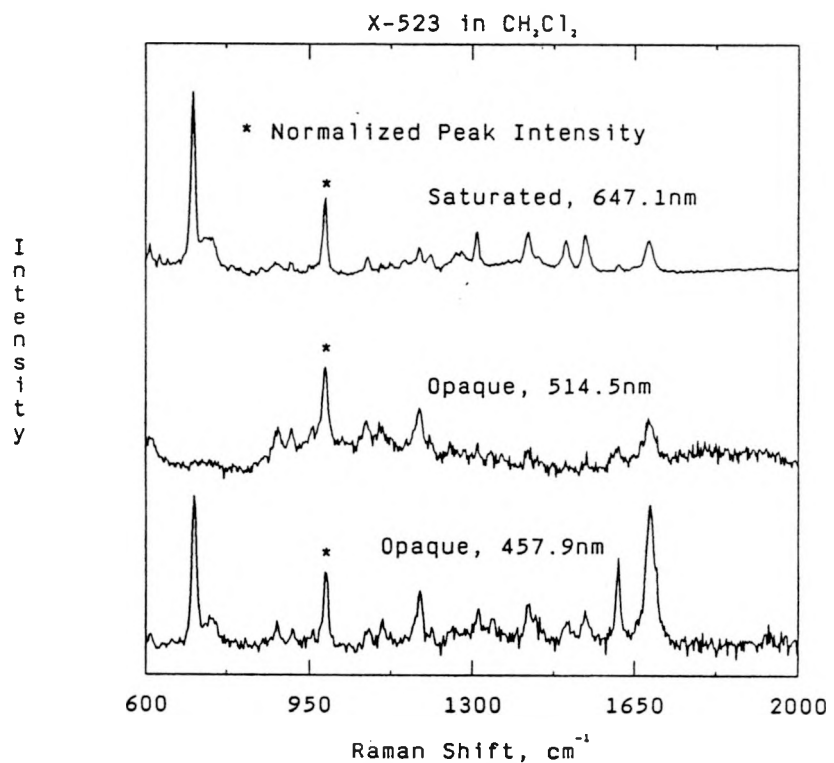


Figure 6. Comparison of non-resonance and resonance Raman spectra of X-523 in methylene chloride. Note the significant enhancement of the  $1683 \text{ cm}^{-1}$  absorption at the 457.9 nm irradiation wavelength.

transition to a charge transfer from the nitrogen of the julolidine (donor) to the carbonyl(s) of the barbituric acid (acceptor). The lack of resonance enhancement of the C=S vibration is evidence that this molecular fragment is not excited in the absorption at 523 nm. This is somewhat surprising because of the large shift in the absorption maximum that occurs upon replacement of the sulfur by an oxygen.

Figures 4 and 5 compare the Raman spectra obtained using four resonant laser wavelengths. In Figure 4 the spectral intensities have been normalized to the 1683  $\text{cm}^{-1}$  band height; in Figure 5 the same spectra are normalized to the height of the 983  $\text{cm}^{-1}$  band. The increase in the intensity of the 704  $\text{cm}^{-1}$  band with decreasing wavelength of irradiation is an indication of the decreased resonance enhancement from the narrow visible absorption peak. The higher frequency Raman modes increase in intensity relative to the lower frequency Raman modes with decreasing laser wavelength. This change in the relative intensities of the Raman bands is probably due to the resonance of a laser frequency with the sum of the visible absorption frequency for the 0  $\rightarrow$  0 transition and the frequency of the Raman transition. The changes in relative intensity are very gradual with respect to laser wavelength and occur over 50 nm rather than the width of a Raman band.

Finally, in Figure 6 Resonance-enhanced spectra are plotted with a nonresonance-enhanced spectrum of X-523 in concentrated  $\text{CH}_2\text{Cl}_2$  solution taken at 647.1 nm. The spectra are normalized to the height of the 983  $\text{cm}^{-1}$  peak. The Raman bands at 983, 1187, 1616 and 1683  $\text{cm}^{-1}$  are significantly and selectively enhanced at 514.9 nm excitation; the bands at 1616  $\text{cm}^{-1}$  and 1683  $\text{cm}^{-1}$  are selectively enhanced with 457.9 nm excitation.

This data shows that the higher Raman frequencies couple with increasing strength to the electronic transition as the laser wavelength decreases and suggests that modifying the chromophore structure to minimize groups with high Raman (vibrational) frequencies may lead to less residual absorption for ADPM SHG.

#### 4. PHASE MATCHED WAVEGUIDES

In order to demonstrate the feasibility of ADPM in a waveguide geometry, thin films of PMMA doped with X-523 were first spun from  $\gamma$ -butyrolactone/propylene glycol methyl ether acetate solutions onto silicon wavers on which several micron thick oxide layers had been grown. The bulk indices of refraction of the films were then determined at 800 and 400 nm from TE mode coupling angles as a function of the concentration of the dye. The difference in index of refraction at these wavelengths (the dispersion) is plotted vs. concentration in Figure 7. Zero dispersion was observed near 6% weight fraction. The absorption coefficient at 400 nm at 6% concentration is 20-25  $\text{cm}^{-1}$ .

The residual absorption of the chromophores at  $2\omega$  limits the theoretical efficiency of SHG using this technique, although thermal effects or slow photochemically induced reactions may be practical challenges. Oudar<sup>5</sup> previously treated the affect of absorption at  $\omega$  or  $2\omega$  on SHG. Under the approximation of zero pump depletion, the efficiency of SHG is given by

$$\eta = \frac{16\pi}{c} I_\omega T_\omega Q_b^2 F$$

where

$$T_\omega = 2 \frac{n}{1+n}$$

$$Q_b = \frac{32\pi^2 d}{\lambda(1+n) \sqrt{\left[ \frac{2\pi}{l_c} \right]^2 + \alpha_{2\omega}^2}}$$

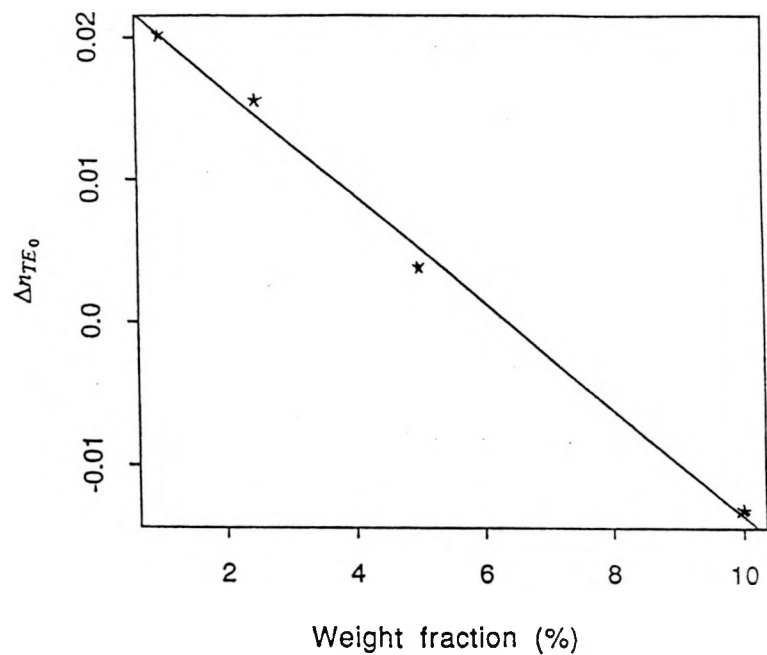


Figure 7. Measured dispersion (effective  $[n(400 \text{ nm}) - n(800 \text{ nm})]$ ) for X-523 doped PMMA slab waveguides as a function of dye concentration.

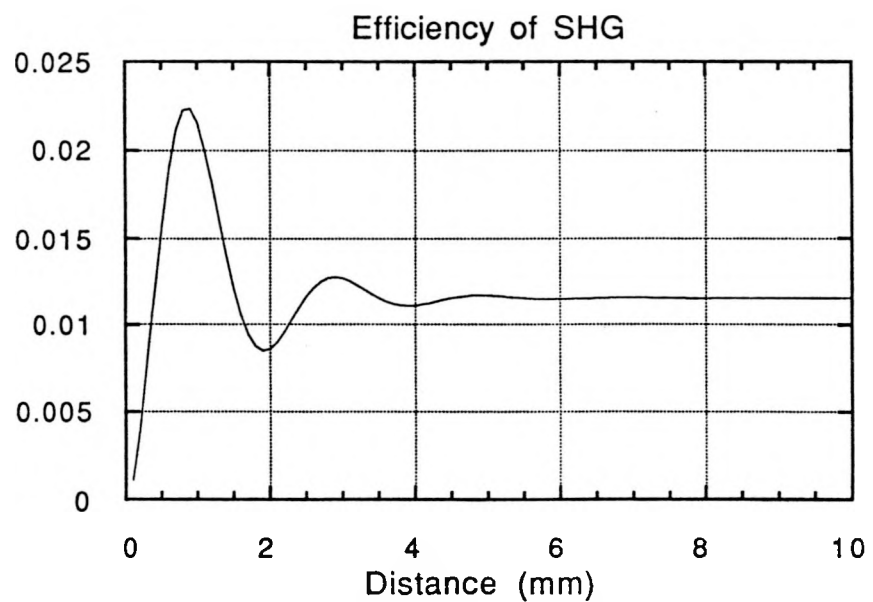


Figure 8. Calculated SHG efficiency of a waveguide doped with NLO dye X-523 at approximately 6% concentration using the parameters listed in Section 4.

$$F = \exp \left[ - \left( \alpha_\omega + \frac{\alpha_{2\omega}}{2} \right) l \right] \left[ \cosh \left( \alpha_\omega - \frac{\alpha_{2\omega}}{2} \right) l - \cos \left( \frac{\pi l}{l_c} \right) \right]$$

In this derivation:	$\eta$	SHG efficiency
	$l$	optical path length
	$l_c$	coherence length
	$\omega$	fundamental frequency
	$\alpha_\omega$	absorption at $\omega$
	$\alpha_{2\omega}$	absorption at $2\omega$
	$d$	NLO coefficient
	$n$	index of refraction
	$I_\omega$	incident intensity

When plotted as a function of path length, the calculated efficiency oscillates and damps to a constant value of approximately 1.2% as shown in Figure 8. Maximum SHG is observed near one coherence length (1 mm). The loss of coherence over length arises from the fact that only over the first 1/e absorption length do the fundamental and second harmonic interfere. At long propagation lengths the constant value of the efficiency is due to the fact that the observed second harmonic is all generated in the last 1/e length. Therefore, even in relatively small devices, efficiencies of greater than 1% may be obtained even from a system which has relatively high absorption at the second harmonic.

### 5. CONCLUSIONS

The large increase in the effective hyperpolarizability associated with the ADPM approach is projected to yield a second harmonic generation efficiency of 1-2% despite the considerable absorbance associated with the dyes currently available. Resonance Raman spectra of one ADPM dye (X-523) suggest that vibronic effects (Franck-Condon factors) contribute significantly to the residual absorption at  $2\omega$  in these dyes. This result indicates that future dye synthesis should target dye structures with relatively small excited state - ground state geometry changes, and/or with rigid chromophores, for improved figures of merit for ADPM SHG.

### 6. ACKNOWLEDGMENTS

A portion of this work was performed at Sandia National Laboratories and was supported by the U.S. Department of Energy under contract DE-AC04-76DP00789. The laboratory efforts of Don Strall, Ron Weagley, Gina Simpson (SNL) and Lori King (AT&T) are gratefully acknowledged.

### 7. REFERENCES

1. P. A. Cahill, K. D. Singer, and L. A. King, "Anomalous-Dispersion Phase-Matched Second Harmonic Generation," *Opt. Lett.* **14**, 1137-1139, 1989.
2. J. A. Armstrong, N. Bloembergen, J. Ducuing, and P. S. Pershan, "Interactions between Light Waves in a Nonlinear Dielectric," *Phys. Rev.* **127**, 1918-1939, 1962.
3. S. R. J. Brueck and H. Kildal, "Efficient Phase-Matched Infrared Third-Harmonic Generation in Liquid CO<sub>2</sub>-SF<sub>6</sub> Mixtures," *Opt. Lett.* **2**, 33-35, 1978.
4. T. Ishiuro, E. Suzuki, A. Y. Hirakawa, and M. Tsuboi, "Resonance Raman Effect in Thiourea," *J. Mol. Spect.* **83**, 360-372, 1980.
5. J. L. Oudar, "Optical Nonlinearities of Conjugated Molecules. Stilbene Derivatives and Highly Polar Aromatic Compounds," *J. Chem. Phys.* **67**, 446-457, 1977.